Molecular Diversity
https://doi.org/10.1007/s11030-020-10039-9

ORIGINAL ARTICLE

New nicotinic acid-based 3,5-diphenylpyrazoles: design, synthesis and antihyperlipidemic activity with potential NPC1L1 inhibitory activity

Mai E. Shoman[1] · Moustafa O. Aboelez[2] · Montaser SH. A. Shaykhon[3] · Sanaa A. Ahmed[4] · Gamal El-Din A. Abuo-Rahma[1] · Omar M. Elhady[5]

Received: 24 November 2019 / Accepted: 18 January 2020

Abstract

Nicotinic acid hydrazide was incorporated into new 4,5-dihydro-5-hydroxy-3,5-diphenylpyrazol-1-yl derivatives. Compounds **6a–h** were synthesized, and their antihyperlipidemic activity was evaluated in high cholesterol diet-fed rat model. Compounds **6e**, **6f** were found to decrease the levels of serum total cholesterol by 14–19% compared to control group. Total triglycerides were also reduced by 24–28% and LDL cholesterol by 16%. As expected from parent niacin, compounds **6e** and **6f** caused an elevation of HDL cholesterol by 33–41%. Docking study supported the ability of designed compounds to block NPC1L1 active site in a manner similar to that observed with ezetimibe.

Keywords 3,5-diphenylpyrazoles · Antihyperlipidemic · Docking · NPC1L1

Introduction

Hyperlipidemia, a condition characterized by elevated levels of one or more plasma lipids [1], is a major risk factor for atherosclerosis and atherosclerosis-associated conditions such as coronary heart diseases (CHD), ischemic cerebrovascular diseases and peripheral vascular diseases. These cardiovascular diseases (CVDs) are considered the cause of more than 30% of total deaths around the world. By 2020, they are expected to be the main cause of death worldwide. A **10**% drop in serum cholesterol level was reported to reduce risk for CHD by 30% [2–4].

One of the oldest antihyperlipidemic agents is niacin [5] (vitamin B3 or nicotinic acid, (**I**)) (Fig. 1). It is known to decrease levels of cholesterol and triglycerides and increase levels of high-density lipoproteins (HDL) [6, 7]. HDL cholesterol levels of > 60 mg/100 mL are considered protective against coronary heart diseases [5], thus niacin is currently having continuous attraction as it has the strongest HDL cholesterol-elevating effect among the drugs currently approved for the modification of lipid levels. Niacin has diverse mechanisms of actions [8]. Niacin inhibits hormone-sensitive lipase [9] and noncompetitively blocks a key enzyme for triglycerides synthesis: diacylglycerol acyltransferase-2 (DGAT-2) [10]. It also reduces the fractional clearance of apo A-1, thus increasing HDL synthesis [2, 8]. Derivatives of nicotinic acid such as nicotinamide and nicotinic acid hydrazide among others also retained the antihyperlipidemic effects of niacin [11, 12]. Several niacin-based drugs were designed and also acquired similar hypolipidemic activity as parent niacin [13, 14].

On the other hand, one more target that can be addressed to lower plasma lipids is Niemann–Pick C1-like 1 protein

Electronic supplementary material The online version of this article (https://doi.org/10.1007/s11030-020-10039-9) contains supplementary material, which is available to authorized users.

✉ Mai E. Shoman
shoman_mai@mu.edu.eg

✉ Gamal El-Din A. Abuo-Rahma
gamal.aborahama@mu.edu.eg

1 Department of Medicinal Chemistry, Faculty of Pharmacy, Minia University, Minia 61519, Egypt

2 Department of Pharmaceutical Chemistry, Faculty of Pharmacy, Sohag University, Sohâg 82524, Egypt

3 Department of Pharmaceutical Chemistry, Faculty of Pharmacy, Al-Azhar University, Assiut 71524, Egypt

4 Department of Pharmacology, Faculty of Medicine, Sohag University, Sohâg 82524, Egypt

5 Department of Chemistry, Sohag University, Sohâg 82524, Egypt

Published online: 17 February 2020

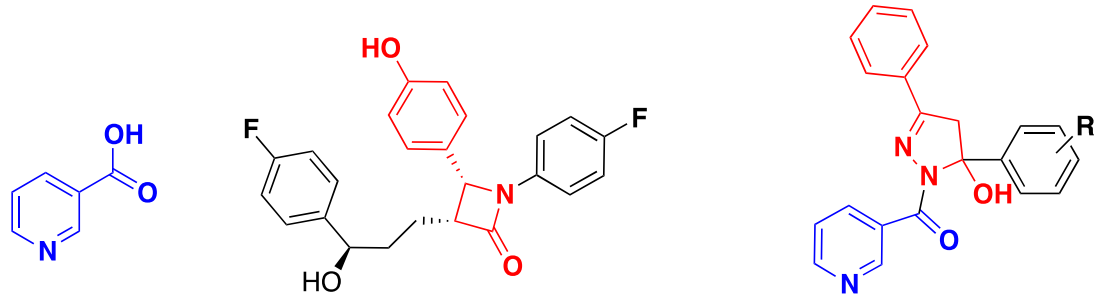

Fig. 1 Structure of nicotinic acid **(I)**, ezetimibe **(II)** and the designed compounds **(6a–h)**

(NPC1L1). NPC1L1 is a transmembrane protein that is found at the enterocytes and hepatocytes [15–17]. It transports sterol for purposes of intestinal cholesterol absorption or hepatobiliary cholesterol excretion. Blockade of NPC1L1 by ezetimibe, (**II**) a β-lactam compound (Fig. 1), leads to hindering cholesterol absorption and hence prevents diet-induced steatosis, obesity and reduces cholesterol level [18]. The hypocholesterolemic drug ezetimibe disrupts the association between NPC1L1 and flotillins, which blocks the formation of the cholesterol-enriched microdomains [19]. 3D structure of NPC1L1 reveals a cholesterol binding site at its *N*-terminal domain with multiple extracellular and intracellular loops, while ezetimibe binds to extracellular domain of C-terminal and leads to disruption of configurational changes required for NPC1L1 activity and binding to cholesterol [17].

One strategy that is currently used in drug design and development is molecular hybridization. It relies on gathering two or more pharmacophoric moieties in one new hybrid. It is usually designed for improving affinity and efficacy, enhancing target selectivity, minimizing adverse effects and introducing different and/or dual modes of action [20, 21]. Herein, we report gathering nicotinic acid and ezetimibe analog in one entity (Fig. 1), replacing 2-azetidinone ring with pyrazoline group, offers an easier synthesis and additional sites for possible interaction with the NPC1L1 receptor. The designed compounds were synthesized and evaluated for their ability to enhance lipid profile and an in silico study was carried out to examine their ability to potentially bind to NPC1L1 active site.

Results and discussion

Chemistry

Synthesis of 5-hydroxylpyrazoles **6a–h** was accomplished through Scheme 1. Claisen–Schmidt condensation reaction of benzaldehyde derivatives **1a–f** and acetophenone derivatives **2a** and **2b** in the presence of NaOH afforded the chalcone derivatives **3a–h** which were identified by their reported melting points (C.f. experimental) [22, 23]. Synthesis of desired 5-hydroxylpyrazoles **6a–h** was done through preparation of the intermediate dibromo derivatives **4a–h.** For preparation of dibromochalcone derivatives **4a–h,** bromine was added in a dropwise manner to the appropriate chalcone derivatives **3a–h** under ice-cooled conditions. The structural formula for dibromochalcone derivatives **4a–h** was proved by their reported melting points (C.f. experimental) [24, 25]. Cyclization of compounds **4a–h** with nicotinic acid hydrazide **5** in the presence of triethylamine (TEA) [26] in refluxing ethanol for 12–24 h afforded the desired hydroxypyrazoles **6a–h**.

A plausible mechanism for the formation of 5-hydroxypyrazolines **6a–h** is illustrated in Fig. 2.

The structures of prepared compounds were substantiated by IR, ^{1}H NMR and ^{13}C NMR spectra as well as elemental microanalyses. IR spectra of compounds **6a–h** showed disappearance of stretching band related to (NH_2) group of nicotinic acid hydrazide and appearance of two bands at 3365–3232 cm^{-1} and 1703–1693 cm^{-1} corresponding to OH group and C=O group, respectively. ^{1}H NMR spectra of compounds **6a–h** showed a singlet signal corresponding to proton of hydroxyl group (OH) at δ 9.21–8.94 ppm that disappeared by deuteration, and the two methylene protons (CH_2) of hydroxylpyrazoline ring appeared as two separate doublets at δ 3.70–3.54 ppm and δ 3.75–3.65 ppm, respectively, with a geminal coupling constant of ($J = 20$ Hz). The appearance of the two doublets clearly reveals the magnetic non-equivalence of the two protons adjacent to a chiral center. The absence of NH and NH_2 absorptions characteristic for the nicotinic acid hydrazide supports the formation of the hydroxypyrazoline **6a–h**. All other protons appear at their expected chemical shifts. Moreover, ^{13}C NMR spectra showed a signal corresponding to C=O group at δ 162–167 ppm, C–OH at δ 81–86 ppm, the methylene carbon

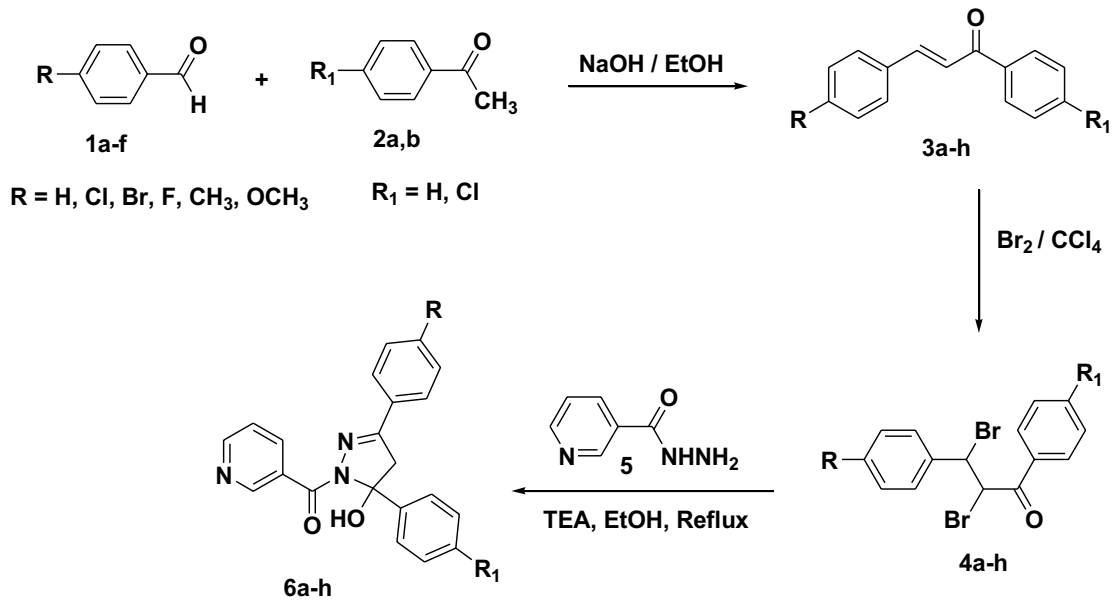

6a: R = R_1 = H; **6b**: R = Cl, R_1 = H; **6c**: R = Br, R_1 = H; **6d**: R = F, R_1 = H; **6e**: R = OCH_3, R_1 = H; **6f**: R = CH_3, R_1 = H; **6g**: R = Cl, R_1 = Cl; **6h**: R = OCH_3, R_1 = Cl

Scheme 1 Synthesis of compounds **6a–h**

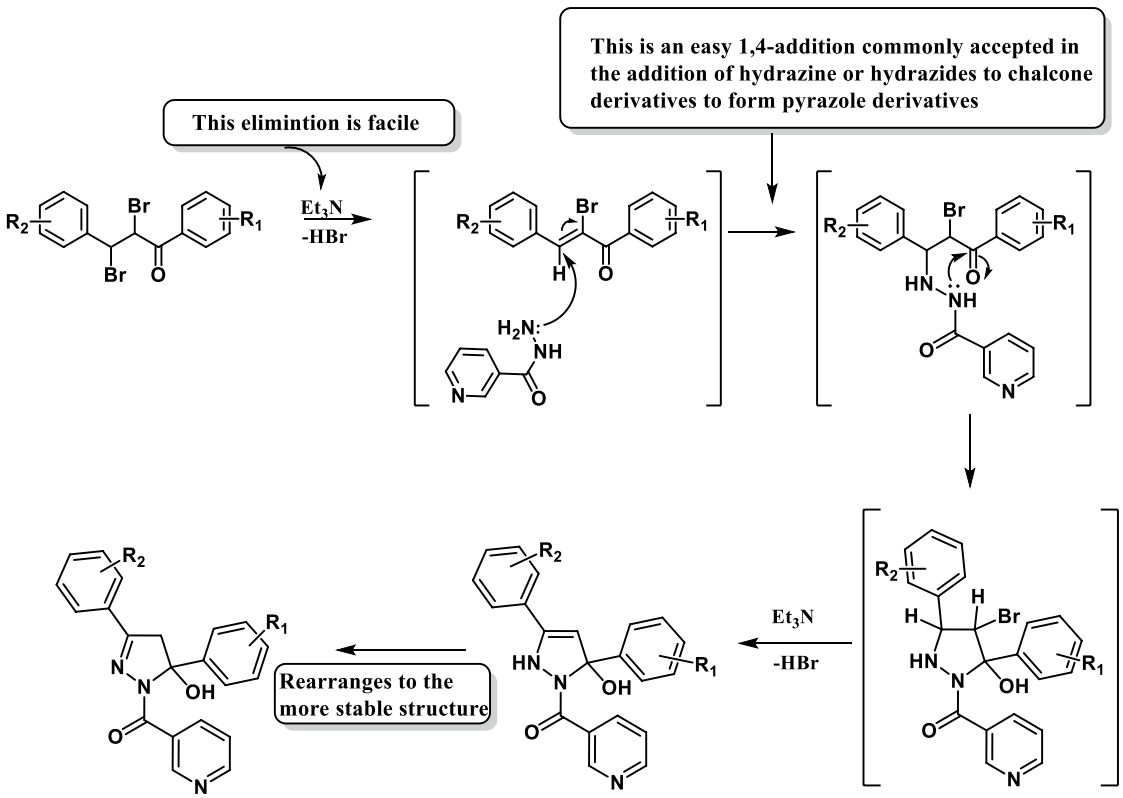

Fig. 2 Plausible mechanism for the synthesis of compounds **6a–h**

$\underline{C}H_2$ of hydroxyl pyrazole at δ 50–54 ppm. All other carbons were observed at their expected chemical shifts. Compounds **6a–h** were obtained as a mixture of both isomers R and S and used for further testing without separation.

Antihyperlipidemic activity

The antihyperlipidemic activity of the synthesized compounds was studied in the high cholesterol diet (HCD)-fed rats model against hyperlipidemic control [i.e., rats fed with HCD and given drug vehicle (0.5% carboxymethylcellulose (CMC) only), by oral administration of 20 mg/Kg of the tested compounds. Hyperlipidemia was induced by feeding rats with HCD (enriched with 2% cholesterol and 1% cholic acid) [27]. Rats receiving normal rodent chow and the drug vehicle (0.5% CMC) served as normal control [28, 29]. Results were compared with those obtained by the reference antihyperlipidemic agent gemfibrozil (Table 1).

The results revealed that feeding rats with high cholesterol diet for 14 days significantly elevated the serum level of TC, TGs and LDL by 56.50%, 68.56% and 101.50%, respectively, when compared with normal control rats. Moreover, induction of hyperlipidemia significantly decreases serum HDL level by 33.55% from that of normal control rats. Cholic acid was added to the high cholesterol diet to increase the response of rats to hyperlipidemia since cholic acid is reported to promote fat and cholesterol absorption from the intestine [28].

The 5-hydroxypyrazoles **6e, 6f** and **6g** significantly reduced the serum level TC of hyperlipidemic rats by 19.45%, 14.7% and 9.17%, respectively, and were more active than the reference gemfibrozil. Moreover, the 5-hydroxypyrazoles **6d** produced comparable antihyperlipidemic activity (5.46%) with the reference. Likewise, no significant reduction in serum TC level was observed in the groups treated with the compounds **6a, 6b** and **6c** (Table 1, Fig. 3).

The 5-hydroxypyrazoles **6e** and **6f** significantly reduced in the serum TG level of the hyperlipidemic rats by 28.77% and 24.45%, respectively; they are more active than the reference gemfibrozil which afforded only 22.68% reduction in serum TG level. Moreover, compounds **6g**, **6b** and **6d** produced mild activity (Table 1, Fig. 4).

Significant elevation of serum level of HDL in hyperlipidemic rats ranging from 33.47% to 41.13% was achieved by the 5-hydroxylpyrazole derivatives **6e** and **6f** than the reference, while compounds **6b**, **6d** and **6g** have comparable activity of standard (20.43%, 17.30% and 21.11%, respectively; Table 1, Fig. 5). Compounds **6e** and **6f** reduced the serum level of LDL of hyperlipidemic rats by percentages ranging from 16% to 16.85% being more active than gemfibrozil (Table 1, Fig. 6).

5-Hydroxylpyrazoles **6e** and **6f** recorded the lowest LDL/HDL ratio (4.13, 4.31). This valuable finding reflects the role of the mentioned compounds in improving the lipid profile preventing the progression of atherosclerosis and subsequent cardiovascular complications [30].

Table 1 Effect of compounds **6a–g**, gemfibrozil and ezetimibe on levels of total cholesterol, total triglycerides, HDL cholesterol and LDL cholesterol measured for hyperlipidemic rats

Groups	TC (mg/dL)	% Fall	TG (mg/dL)	% Fall	HDL-C (mg/dL)	% Rise	LDL-C (mg/dL)	% Fall	LDL/HDL
Control	71.83 ± 1.50		50.00 ± 1.14		18.56 ± 1.52		39.50 ± 2.71		2.13
HCD fed	115.33 ± 1.60		92.50 ± 0.71		11.50 ± 0.50		80.00 ± 1.91		6.69
HCD fed + gemfibrozil	109.50 ± 6.27	4.65	71.52 ± 3.04**	22.68	14.50 ± 0.52**	25.54	75.89 ± 7.24*	5.13	5.23
HCD fed + Ezetimibe[c]	52.39 + 5.18	54.57	34.26 + 5.37	62.5	31.50 + 3.83	265.21			
HCD fed + **6a**	117.40 ± 2.40**	− 1.79[b]	95.90 ± 3.81**	− 3.67[b]	11.15 ± 1.43**	− 3.04[b]	81.50 ± 2.90**	− 1.87[c]	7.31
HCD fed + **6b**	112.00 ± 3.80**	2.88	78.65 ± 6.82**	14.97	13.85 ± 2.63**	20.43	78.77 ± 3.60**	1.53	5.68
HCD fed + **6c**	115.22 ± 1.24	− 1.04[b]	93.48 ± 2.62	− 1.05[b]	10.55 ± 0.52	− 8.65[b]	83.49 ± 3.30	− 2.48[c]	7.77
HCD fed + **6d**	110.77 ± 0.40**	5.46	81.57 ± 4.90**	11.81	13.55 ± 1.02**	17.30	76.05 ± 4.50*	4.93	5.61
HCD fed + **6e**	92.89 ± 1.10**	19.45	65.88 ± 3.34**	28.77	16.25 ± 1.03**	41.13	67.20 ± 2.34	16.11	4.13
HCD fed + **6f**	98.33 ± 3.40**	14.71	69.88 ± 2.83**	24.45	15.35 ± 1.32**	33.47	66.52 ± 2.80*	16.85	4.31
HCD fed + **6g**	104.75 ± 5.70**	9.17	76.82 ± 7.90**	16.19	13.99 ± 0.50**	21.11	76.99 ± 4.23*	3.70	5.52

Results expressed as the mean of three different measurements ± standard error of mean

TC Total cholesterol, *TG* triglycerides, *HDL-C* high-density lipoprotein cholesterol, *LDL-C* low-density lipoprotein cholesterol

*Significantly different from hyperlipidemic control group at $P < 0.05$

**Significantly different from hyperlipidemic control group at $P < 0.01$

[a]Reduction in the level of serum TC or TG is calculated for groups as percentage from the hyperlipidemic control group

[b]Negative values indicate increase in the level of serum TC or TG

[c]Ezetemibe data were obtained from previous report [31]

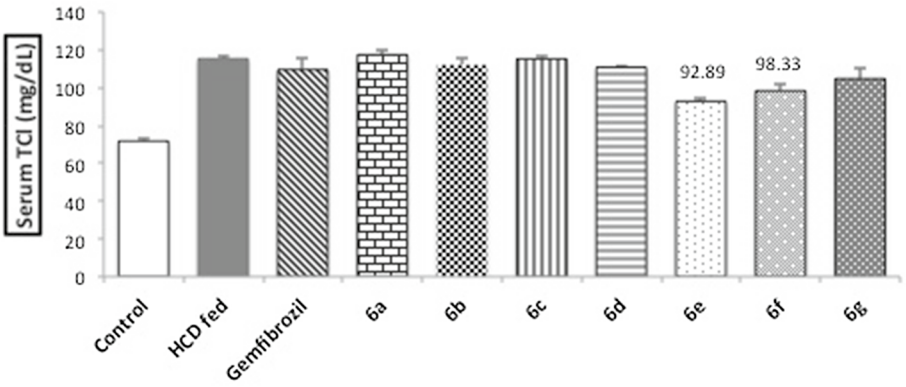

Fig. 3 Effect of compounds **6a–g** and gemfibrozil on serum total cholesterol of hyperlipidemic rats

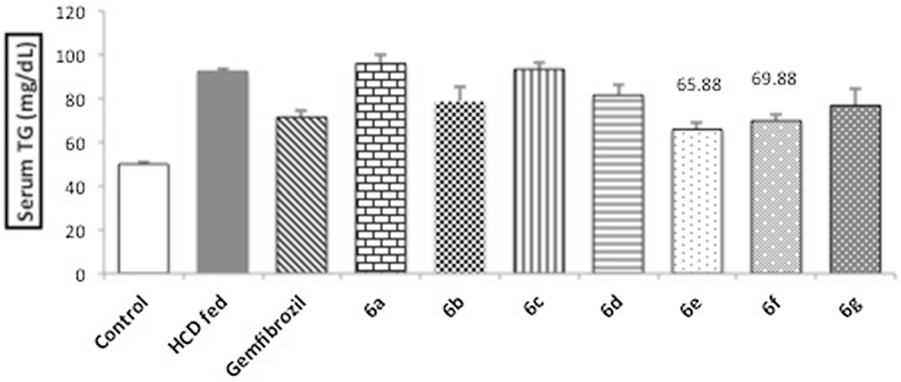

Fig. 4 Effect of the compounds **6a–g** and gemfibrozil on serum triglyceride level of hyperlipidemic rats

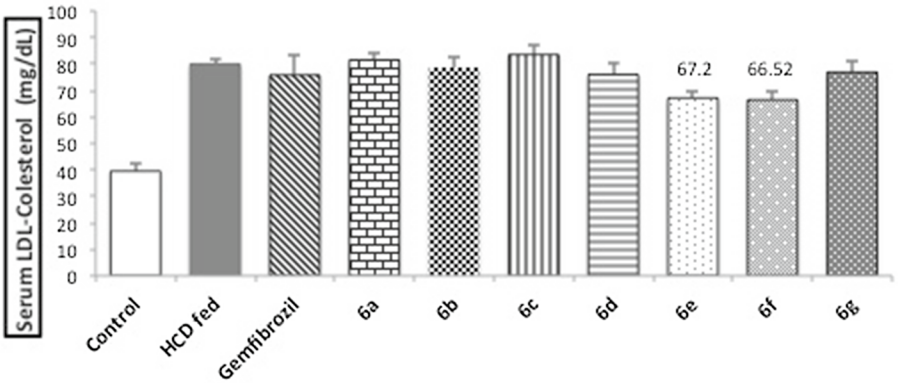

Fig. 5 Effect of the compounds **6a–g** and gemfibrozil on serum LDL cholesterol of hyperlipidemic rats

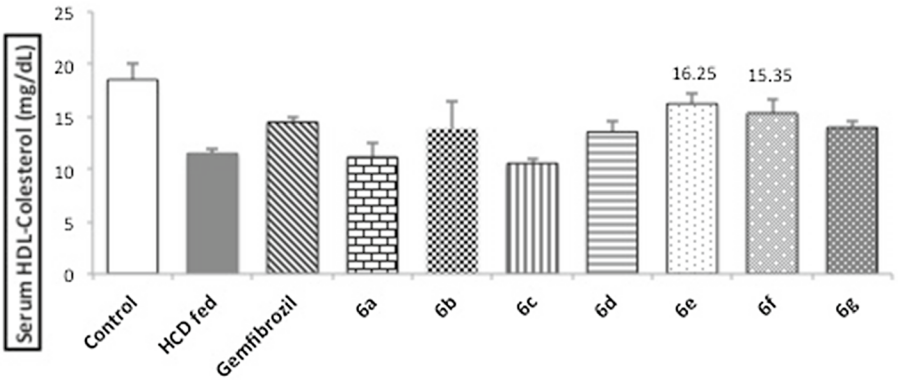

Fig. 6 Effect of the compounds **6a–g** and gemfibrozil on serum HDL cholesterol of hyperlipidemic rats

In conclusion, the analysis of the lipid profile data (TC, TG, HDL and LDL) of different groups clearly suggests that some of the synthesized compounds exerted good hypolipidemic activity. The 5-hydroxypyrazoles **6e** and **6f** appear to be good hypolipidemic agents acting via several mechanisms. They produced striking reduction in serum levels of TC, TG, LDL and elevation of serum HDL with lowered LDL/HDL ratios. Compounds **6e** and **6f** with *p*-methyl and *p*-methoxy of 3-phenyl are the best compounds among this group suggesting a role for an electron-donating group on this phenyl ring that might contribute to the increase in the strength of the interaction with the essential amino acid HIS 124 in the active site of NPC1L1 (c.f. molecular docking section).

Molecular docking study

Docking of compounds **6a–h** (both enantiomers) and ezetimibe (Fig. 7) into the active site of Niemann–Pick C1-like 1 protein (NPC1L1, pdb code: 3QNT) was performed using MOE program. Compounds gave very stable complexes with enzyme active site (energy score − 10.3 to − 11.9; Table 2), and this fact supports our hypothesis that part of the antihyperlipidemic activity observed may be attributed to blocking cholesterol absorption by NPC1L1 enzyme. All compounds fitted in the ezetimibe binding site at N-terminal domain of the enzyme [31]. Comparing the docking results for the two enantiomers found for the tested compounds generally revealed that the R isomer forms more stable complexes (E scores = −7.89 for S isomer of compound **6f** and − 11.3 for the R isomer). R isomers also showed better interaction than the corresponding S isomer. While the R isomer of both compounds **6e** and **6f** with the highest antihyperlipidemic activity possibly formed three stable interactions with amino acid residues in NPC1L1 active site (Figs. 8, 9), the S isomer formed a single pi–pi interaction with HIS 124 (Fig. 10), suggesting a better potency for the R isomer.

Moreover, the tested compounds showed similar interactions compared to those observed with ezetimibe supporting the hypothesis that both share a similar mechanism of action as inhibitors of NPC1L1. All compounds were found to interact with HIS 124 which is reported to be an essential residue in NPC1L1 active site [31]. Though all compounds form stable complexes at the active site, that does not explain the variable in vivo activity observed. Amount of interaction done can offer such explanation. Compounds 6e and 6f showing the highest antihyperlipidemic activity showed also the highest amount of interaction suggested with NPC1L1 active site. Compounds **6e** and 6**f** both bonded to both amino acids with significant H-bond of 2.6–2.7 Å with THR 128 and *pi–pi* interactions of length 3.8–3.9 Å with HIS 124. The two compounds make an additional hydrogen bond to GLN 95 for compound **6e** and SER 56 for **6f**. The rest of compounds showed one possible *pi–pi* interaction with HIS 124 with or without a hydrogen bond formation. The importance of the presence of electron-donating group in both active compounds might be reflecting a higher electron density on the attached phenyl group resulting in tighter interaction with HIS 124.

Results also showed that although the *R* enantiomers of compounds **6a–h** introduce more stable complexes than that of ezetimibe, using a mixture of both *R* and *S* (which showed theoretical weaker binding to NPC1L1) might account for the lower activity observed. Other pharmacokinetic parameters also might account for that and thus requires further testing.

In summary, the hydroxypyrazoles designed can be considered promising candidates for the treatment of hyperlipidemia through inhibition of NPC1L1 though further testing is still required including in vitro testing and assessment of pharmacokinetic parameters in in vivo model.

Conclusion

New 5-hydroxypyrazoles derivatives were prepared, and their antihyperlipidemic activity was screened in induced hyperlipidemic rats. Among the synthesized compounds, **6e** and **6f** were found to be the most active antihyperlipidemic agent affording significant hypocholesterolemic and hypotriglyceridemic activities. Compounds **6e** and **6f** reduced TC by 14 and 19%, and reduced total glycerides by 24 and 28%, respectively. Also, the LDL cholesterol was reduced by 16%. Interestingly, compounds **6e** and **6f** experienced an elevation of HDL cholesterol by 33 and 41%, respectively. Virtual docking study into NPC1L1 active site revealed that these compounds have the ability to block NPC1L1 active site in a manner similar to that observed with ezetimibe. Testing both enantiomers of 6e and 6f, the R enantiomer showed more stable complexes and better interaction with residues in the active site of NPC1L1 more than the S enantiomer. The 5-hydroxypyrazoles derivatives **6e**, **6f** seem to be a good candidate for developing a new strong derivative with good antihyperlipidemic and antiatherosclerotic benefits.

Experimental

Chemistry

All melting points were recorded on Melt-Temp II melting point apparatus. IR spectra were measured as Bruker Alpha Fourier Transform (FT-IR). 1H-NMR and

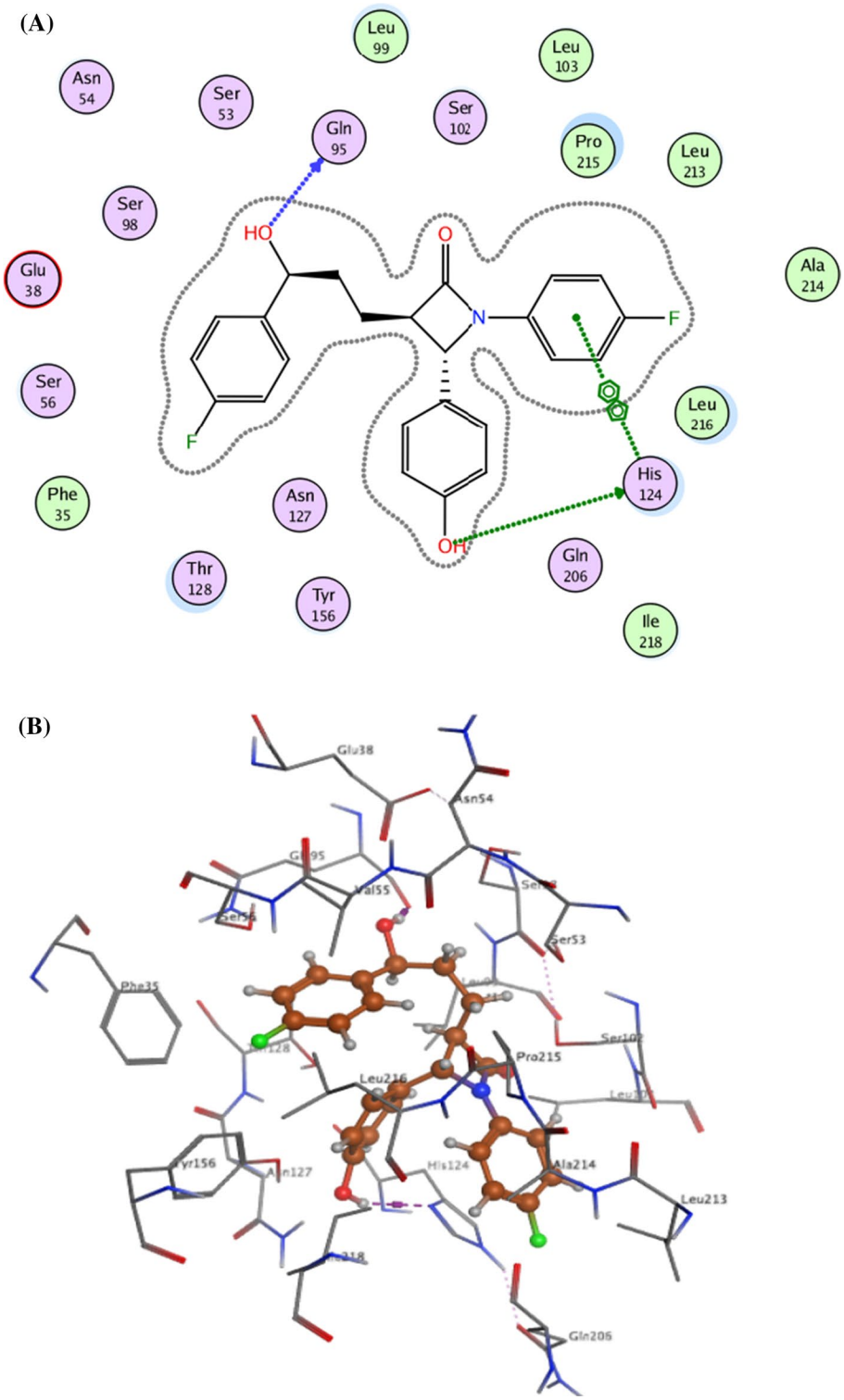

Fig. 7 (**A**) 2D drawings and (**B**) 3D drawing of ezetimibe docked into active sites of NPC1L1 (pdb: 3QNT) showing interactions with different amino acid residues found in the active site

13C-NMR spectra were recorded on a Bruker at 400 MHz using TMS as an internal reference and DMSO-*d6* as a solvent. [Chemical shift (δ) values are expressed in parts per million (ppm).] The elemental analyses were carried out on a PerkinElmer 240C Microanalyzer. All compounds were checked for their purity on TLC plates.

Table 2 Types of interactions and energy scores for the complexes formed from compounds **6a–h** (*R* isomer) at the active sites of NPC1L1 (pdb: 3QNT) studied using MOE 2014

Comp. #	Energy score	Interaction		
		Receptor	Type	Length (Å)
6a	− 10.6907	GLN 95	H-bond	4.44
		HIS 124	pi–pi	3.86
6b	− 10.3158	THR 128	H-bond	2.69
		HIS 124	pi–pi	3.67
6c	− 11.3639	HIS 124	pi–pi	3.48
		GLN 206	H-bond	3.83
6d	− 11.920	HIS 124	pi–pi	3.78
6e	− 10.71	GLN 95	H-bond	3.39
		THR 128	H-bond	2.62
		HIS 124	pi–pi	3.84
6f	− 11.33	SER 56	H-bond	2.92
		THR 128	H-bond	2.71
		HIS 124	pi–pi	3.89
6g	− 10.7410	GLU 38	H-bond	3.43
		HIS 124	pi–pi	3.99
6h	− 10.7699	GLU 38	H-bond	3.09
		HIS 124	pi–pi	3.94
Ezetimibe	− 8.79	HIS 124	H-bond	3.09
		HIS 124	pi–pi	3.96
		GLN 95	H-bond	2.9

General procedure for synthesis of (4,5-dihydro-5-hydroxy-3,5-diphenylpyrazol-1-yl) (pyridin-3-yl)methanone derivatives (6a–h)

Nicotinic acid hydrazide **5** (1.37 g, 0.01 mol) was added to a solution of the appropriate dibromochalcone derivatives **4a–h** (0.01 mol) in absolute ethanol (30 mL). Triethylamine (2 mL) was added to the mixture. The reaction mixture was heated at reflux for 12–24 h. The progress of the reaction was monitored by TLC using hexane/ethyl acetate (7:3) as an eluent. The volume of the solution was reduced, cooled, poured on crushed ice and kept overnight. The precipitated was washed successively with water, filtered off, dried and recrystallized from ethanol to get 5-hydroxypyrazoles **6a–h.**

5-Hydroxy-3,5-diphenyl-4,5-dihydro-1*H*-pyrazol-1-yl(pyridin-3-yl) methanone 6a White crystals; yield (2.25 g, 66%), mp 188–190 °C; IR (KBr) $\tilde{\upsilon}$ (cm^{-1}): 3361.35 (OH), 3161.66 (Ar–H), 1694.05 (C=O), 1595.68 (C=N), 1532.58 (C=C); ^{1}H NMR (DMSO-d_6) δ: 9.21 (*s*, 1H, OH; exchangeable with D_2O), 8.81 (*s*, 1H, pyridyl-H-2), 8.27 (*d*, 1H, *J* = 8 Hz, pyridyl-H-6), 7.97 (*d*, 1H, *J* = 8 Hz, pyridyl-H-5), 7.85 (*d*, 1H, *J* = 8 Hz, pyridyl-H-4), 7.74 (*d*, *J* = 8 Hz, 2H, Ar–H), 7.58 (*d*, 2H, *J* = 8 Hz, Ar–H), 7.39 (*t*, 3H, *J* = 8 Hz, Ar–H), 7.32–7.29 (*m*, 3H, Ar–H), 3.72 (*d*, 1H, *J* = 20 Hz, pyrazoline-CH$_2$), 3.59 (*d*, 1H, *J* = 20 Hz, pyrazoline-CH$_2$); ^{13}C NMR (DMSO-d_6) δ: 162.96, 153.47, 151.21, 150.87, 142.76, 137.25, 136.50, 132.56, 130.97, 130.07, 128.81, 128.25, 127.80, 125.18, 122.98, 85.18, 50.89; Anal. calcd for $C_{21}H_{17}N_3O_2$ (343.13): C, 73.45; H, 4.99; N, 12.24, found: C, 73.35; H, 4.97; N, 12.32.

3-(4-Chlorophenyl)-5-hydroxy-5-phenyl-4,5-dihydro-1*H*-pyrazol-1-yl (pyridin-3-yl)methanone 6b White crystals; yield (2.25 g, 60%), mp 178–180 °C; IR (KBr) $\tilde{\upsilon}$ (cm^{-1}): 3365.13 (OH), 3159.45 (Ar–H), 1693.54 (C=O), 1597.84 (C=N), 1535.58 (C=C); ^{1}H NMR (DMSO-d_6) δ: 9.19 (s, 1H, OH; exchangeable with D_2O), 8.79 (*s*, 1H, pyridyl-H-2), 8.20 (*d*, 1H, *J* = 8 Hz, pyridyl-H-6), 7.89 (*d*, 1H, *J* = 8 Hz, pyridyl-H-5), 7.86 (*d*, 1H, *J* = 8 Hz, pyridyl-H-4), 7.73 (*d*, *J* = 8 Hz, 2H, Ar–H), 7.58 (*d*, 2H, *J* = 8 Hz, Ar–H), 7.39 (*t*, 3H, *J* = 8 Hz, Ar–H), 7.31(*d*, *J* = 8 Hz, 2H, Ar–H), 3.70 (*d*, 1H, *J* = 20 Hz, pyrazoline-CH$_2$), 3.57 (*d*, 1H, *J* = 20 Hz, pyrazoline-CH$_2$); ^{13}C NMR (DMSO-d_6) δ: 164.36, 152.72, 151.71, 150.27, 143.76, 138.25, 135.50, 131.56, 131.07, 129.37, 128.81, 128.03, 126.80, 125.18, 121.56, 84.32, 50.19; Anal. calcd for $C_{21}H_{16}ClN_3O_2$ (377.09): C, 66.76; H, 4.27; N, 11.12, found: C, 66.61; H, 4.39; N, 11.20.

3-(4-Bromophenyl)-5-hydroxy-5-phenyl-4,5-dihydro-1*H*-pyrazol-1-yl (pyridin-3-yl)methanone 6c Colorless solid; yield (2.73 g, 64%); mp 152–154 °C; IR (KBr) $\tilde{\upsilon}$ (cm^{-1}): 3272.13 (OH), 3163.50 (Ar–H), 1699.79 (C=O), 1597.84 (C=N), 1535.58 (C=C); ^{1}H NMR (DMSO-d_6) δ: 8.98 (s, 1H, OH; exchangeable with D_2O), 8.71 (*s*, 1H, pyridyl-H-2), 8.18 (*d*, 1H, *J* = 4 Hz, pyridyl-H-6), 7.91 (*d*, 1H, *J* = 8 Hz, pyridyl-H-5), 7.86 (*d*, 1H, *J* = 8 Hz, pyridyl-H-4), 7.73 (*d*, *J* = 8 Hz, 2H, Ar–H), 7.58 (*d*, 2H, *J* = 8 Hz, Ar–H), 7.40 (*d*, 2H, *J* = 8 Hz, Ar–H), 7.34–7.29(*m*, 3H, Ar–H), 3.69 (*d*, 1H, *J* = 20 Hz, pyrazoline-CH$_2$), 3.59 (*d*, 1H, *J* = 20 Hz, pyrazoline-CH$_2$); ^{13}C NMR (DMSO-d_6) δ: 160.56, 152.82, 151.76, 150.27, 142.71, 137.27, 135.53, 132.49, 131.44, 130.39, 129.38, 128.83, 128.44, 127.34, 123.48, 82.48, 51.65; Anal. calcd for $C_{21}H_{16}BrN_3O_2$ (421.04): C, 59.73; H, 3.82; N, 9.95, found: C, 59.60; H, 3.66; N, 9.79.

3-(4-Fluorophenyl)-5-hydroxy-5-phenyl-4,5-dihydro-1*H*-pyrazol-1-yl (pyridin-3-yl)methanone 6d White crystals; yield (2 g, 55%); m.p. 217–218 °C; IR (KBr) $\tilde{\upsilon}$ (cm^{-1}): 3312.13 (OH), 3031.79 (Ar–H), 1696.95 (C=O), 1597.84 (C=N), 1529.58 (C=C); ^{1}H NMR (DMSO-d_6) δ: 9.11 (*s*, 1H, OH; exchangeable with D_2O), 8.84 (*s*, 1H, pyridyl-H-2), 8.30 (*d*, 1H, *J* = 4 Hz, pyridyl-H-6), 7.78 (*d*, 1H, *J* = 4 Hz, pyridyl-H-5), 7.65 (*d*, 1H, *J* = 4 Hz, pyridyl-H-4), 7.56 (*d*, *J* = 8 Hz, 2H, Ar–H), 7.46 (*d*, 2H, *J* = 8 Hz, Ar–H), 7.38 (*d*, 2H, *J* = 8 Hz, Ar–H), 7.32–7.29(*m*, 3H, Ar–H), 3.72

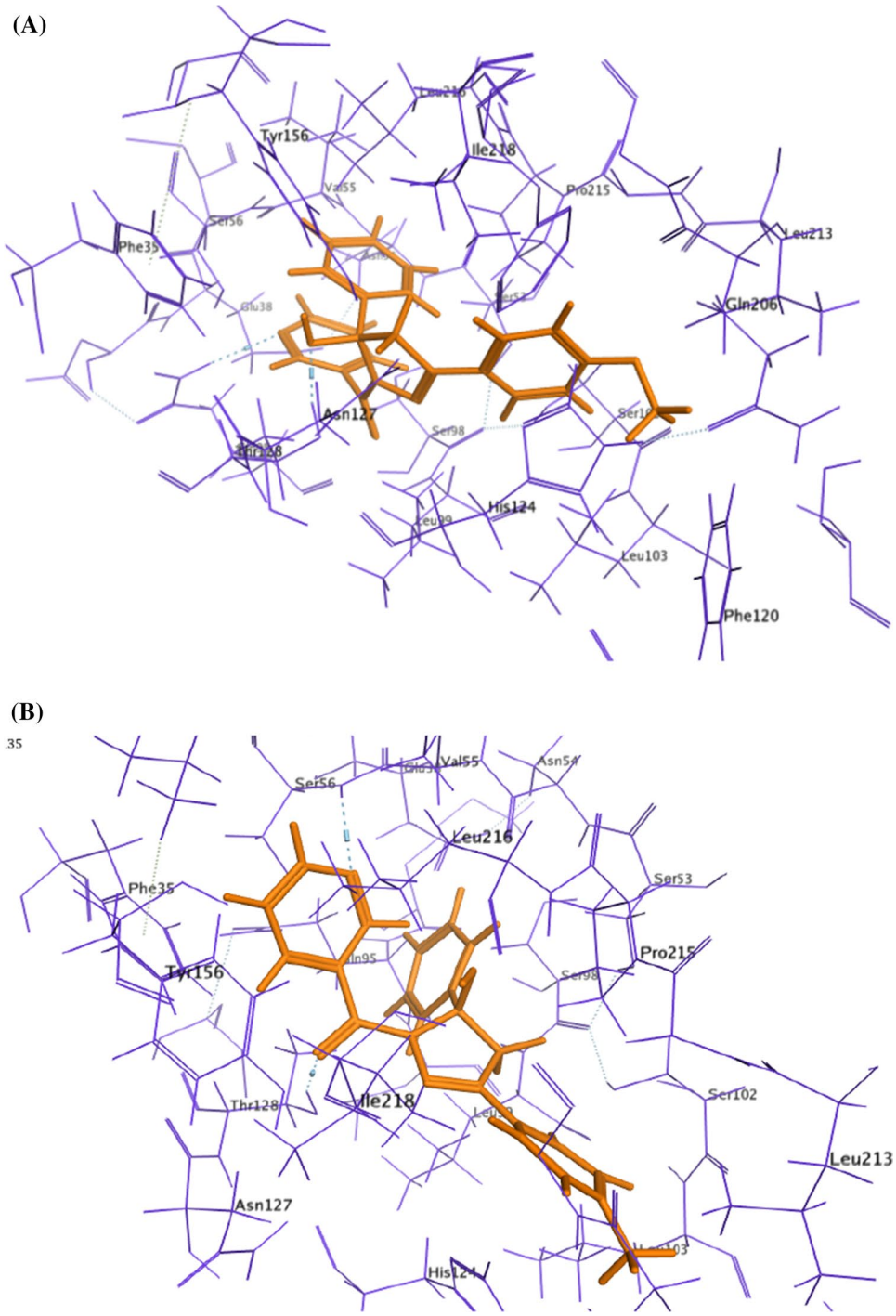

Fig. 8 3D drawings of the R isomer of (**A**) compound **6e** and (**B**) compound **6f** docked into active sites of NPC1L1 (pdb: 3QNT) showing interactions with different amino acid residues found in the active site

(*d*, 1H, *J* = 20 Hz, pyrazoline-C$\underline{H}_2$), 3.57 (*d*, 1H, *J* = 20 Hz, pyrazoline-C$\underline{H}_2$); ^{13}C NMR (DMSO-d_6) *δ*: 162.71, 153.12, 152.76, 150.27, 145.53, 139.13, 136.15, 132.49, 131.71, 130.39, 129.82, 129.13, 128.44, 125.53, 122.71, 81.44, 50.14; Anal. Calcd for $C_{21}H_{16}FN_3O_2$ (361.12) : C, 69.80; H, 4.46; N, 11.63. Found: C, 69.67; H, 4.38; N, 11.51.

5-Hydroxy-3-(4-methoxyphenyl)-5-phenyl-4,5-dihydro-1*H*-pyrazol-1-yl (pyridin-3-yl)methanone 6e Pale yellow crystals; yield (2.25 g, 60%); mp 158–160 °C; IR (KBr) υ (cm^{-1}): 3259.67 (OH), 3021.99 (Aliph.-H), 1695.87 (C=O), 1590.84 (C=N), 1535.58 (C=C); ^{1}H NMR (DMSO-d_6) *δ*: 8.97 (*s*, 1H, O$\underline{H}$; exchangeable with D_2O), 8.79 (*s*, 1H, pyridyl-H-2), 8.17 (*d*, 1H, *J* = 4 Hz, pyridyl-H-6), 7.78 (*d*, 1H, *J* = 8 Hz, pyridyl-H-5), 7.70 (*d*, 1H, *J* = 8 Hz, pyridyl-H-4), 7.56 (*d*, *J* = 8 Hz, 2H, Ar–H), 7.50 (*d*, 2H, *J* = 8 Hz, Ar–H), 7.42 (*d*, 2H, *J* = 8 Hz, Ar–H), 7.31 (*t*, 3H, *J* = 8 Hz, Ar–H), 3.99 (*s*, 3H, OC$\underline{H}_3$), 3.70 (*d*, 1H, *J* = 20 Hz,

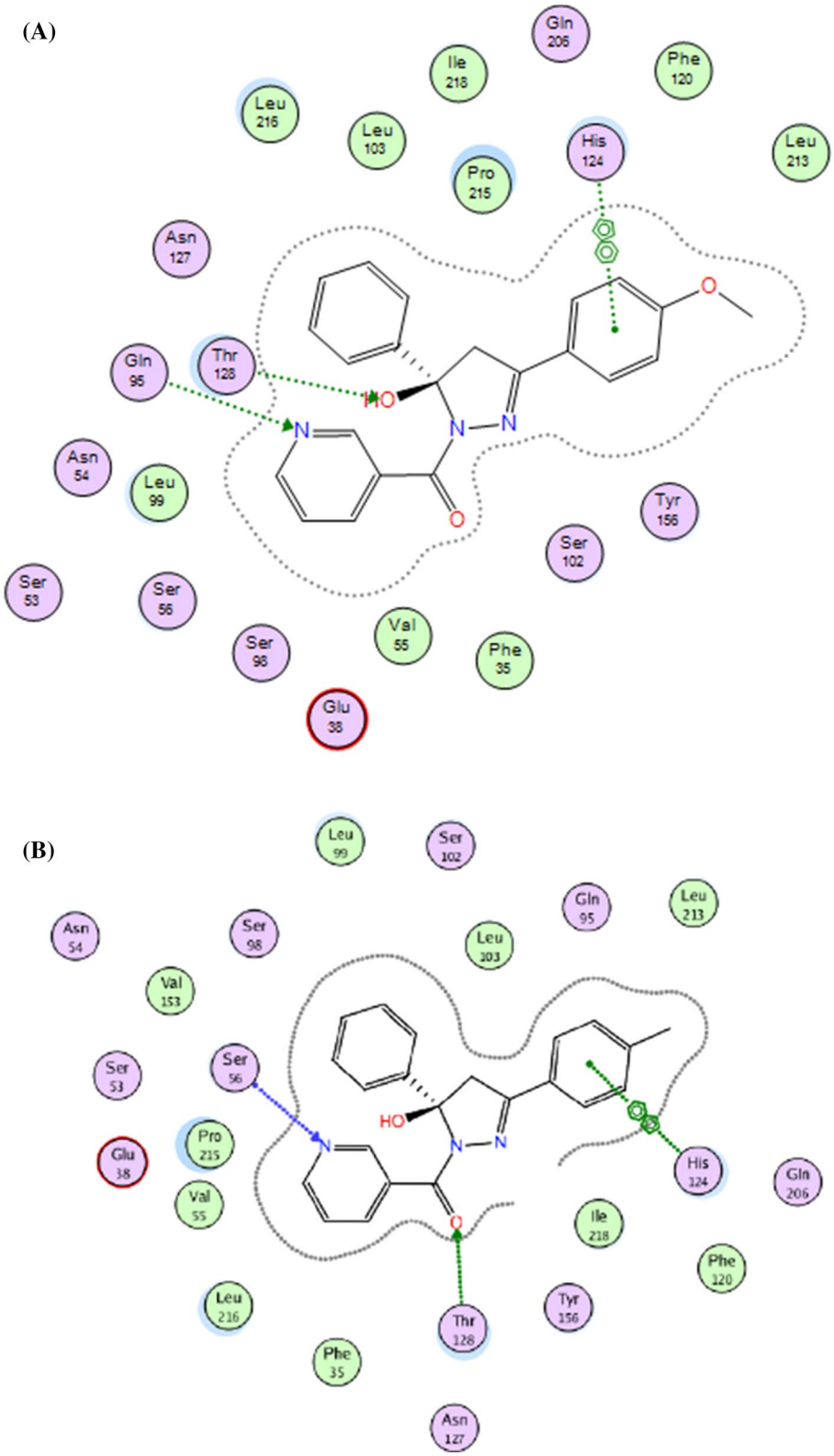

Fig. 9 2D drawings of the R isomer of (**A**) compound **6e** and (**B**) compound **6f** docked into active sites of NPC1L1 (pdb: 3QNT) showing interactions with different amino acid residues found in the active site

pyrazoline-C$\underline{H}_2$), 3.57 (*d*, 1H, $J = 20$ Hz, pyrazoline-C$\underline{H}_2$); ^{13}C NMR (DMSO-d_6) δ: 165.80, 156.56, 152.21, 151.87, 145.76, 138.25, 136.50, 134.56, 133.47, 130.07, 129.81, 129.21, 126.50, 125.18, 122.47, 81.47, 52.21, 50.60; Anal. calcd for $C_{22}H_{19}N_3O_3$ (373.14): C,70.76; H, 5.13; N, 11.25, found C, 70.58; H, 5.22; N, 11.12.

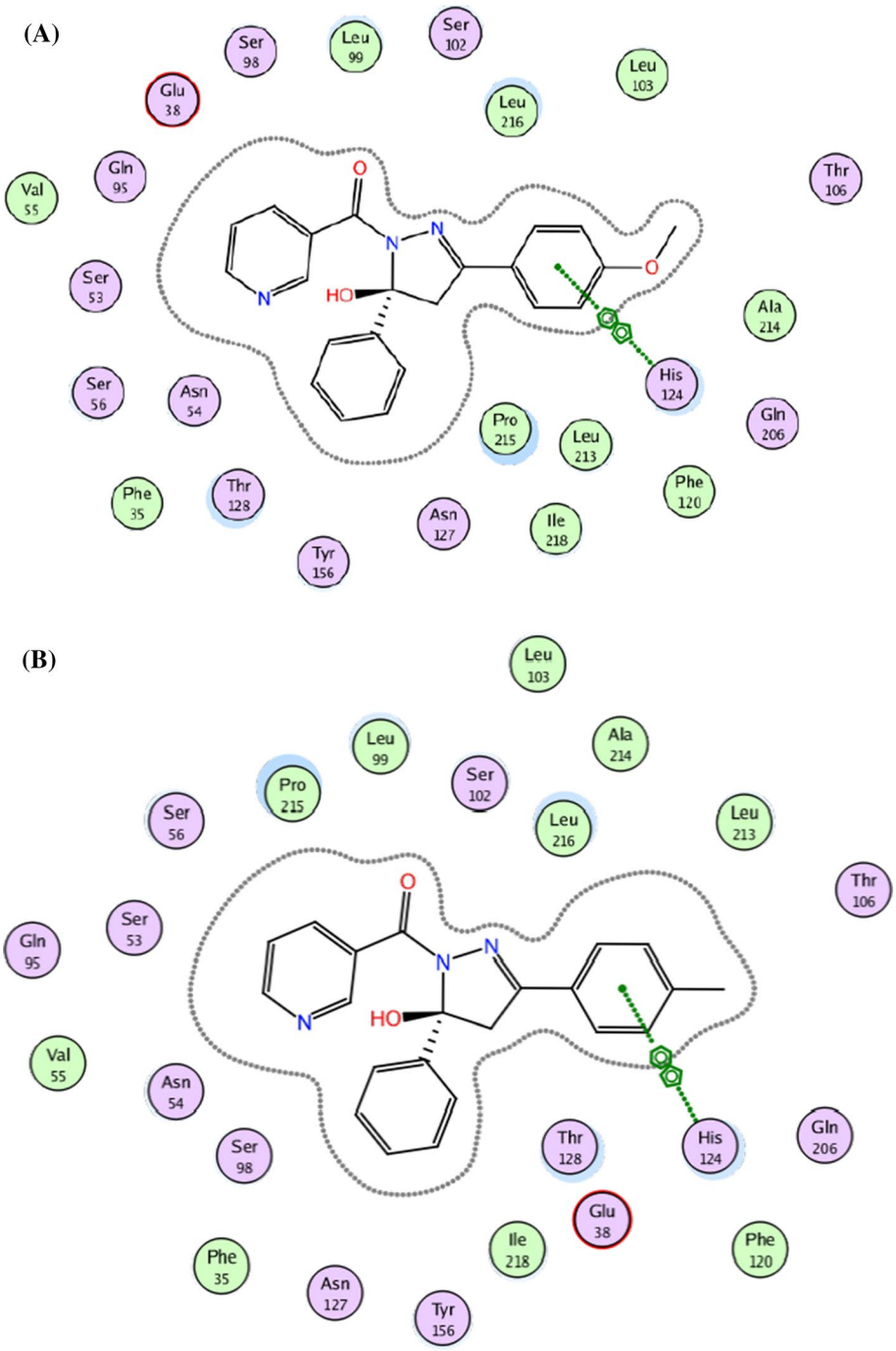

Fig. 10 2D drawings of the S enantiomer of (**A**) compound **6e** and (**B**) compound **6f** docked into active sites of NPC1L1 (pdb: 3QNT) showing interactions with different amino acid residues found in the active site

5-Hydroxy-5-phenyl-3-*p*-tolyl-4,5-dihydro-1*H*-pyrazol-1-yl(pyridin-3-yl)methanone 6f Pale yellow crystals; yield (1.95 g, 55%); mp 181–183 °C; IR(KBr) ὺ (cm^{-1}): 3299.13 (OH), 3027.99 (Ar–H), 1695.93 (C=O), 1590.84 (C=N), 1535.58 (C=C); ^{1}H NMR (DMSO-d_6) δ: 8.94 (*s*, 1H, OH; exchangeable with D_2O), 8.70 (*s*, 1H, pyridinyl-H-2), 8.19 (*d*, 1H, $J=4$ Hz, pyridinyl-H-6), 7.80 (*d*, 1H, $J=8$ Hz, pyridinyl-H-5), 7.70 (*d*, 1H, $J=8$ Hz, pyridinyl-H-4), 7.58 (*d*, $J=8$ Hz, 2H, Ar–H), 7.50 (*d*, 2H, $J=8$ Hz, Ar–H), 7.41–7.35 (*m*, 3H, Ar–H), 7.30 (*d*, 2H, $J=8$ Hz, Ar–H), 3.68 (*d*, 1H, $J=20$ Hz, pyrazoline-CH$_2$), 3.57 (*d*, 1H, $J=20$ Hz, pyrazoline-CH$_2$), 2.41 (*s*, 3H, CH$_3$); ^{13}C NMR (DMSO-d_6) δ: 167.80, 153.47, 152.21, 150.87, 144.76, 138.25, 136.50, 134.56, 133.21, 132.21, 128.81, 128.18, 127.80, 126.18, 123.47, 83.47, 53.67, 23.97; Anal. calcd for $C_{22}H_{19}N_3O_2$ (357.15): C, 73.93; H, 5.36; N, 11.76, found C, 73.80; H, 5.21; N, 11.64.

3,5-Bis(4-chlorophenyl)-5-hydroxy-4,5-dihydro-1*H*-pyrazol-1-yl) (pyridin-3-yl)methanone 6g Colorless solid; yield (2.4 g, 58%); mp 209–211 °C; IR (KBr) $\tilde{\upsilon}$ (cm^{-1}): 3232.13 (OH), 3031.99 (Ar–H), 1694.78 (C=O), 1590.84 (C=N), 1535.58 (C=C); ^{1}H NMR (DMSO-d_6) δ: 9.17 (*s*, 1H, OH; exchangeable with D_2O), 8.79 (*s*, 1H, pyridyl-H-2), 8.22 (*d*, 1H, $J=4$ Hz, pyridyl-H-6), 7.89 (*d*, 1H, $J=8$ Hz, pyridyl-H-5), 7.86 (*d*, 1H, $J=8$ Hz, pyridyl-H-4), 7.73 (*d*, $J=8$ Hz, 2H, Ar–H), 7.58 (*d*, 2H, $J=8$ Hz, Ar–H), 7.40 (*d*, 2H, $J=8$ Hz, Ar–H), 7.30 (*d* 2H, $J=8$ Hz, Ar–H), 3.70 (*d*, 1H, $J=20$ Hz, pyrazoline-CH_2), 3.55 (*d*, 1H, $J=20$ Hz, pyrazoline-CH_2); ^{13}C NMR (DMSO-d_6) δ: 162.76, 153.47, 152.21, 150.87, 142.76, 138.25, 136.50, 134.56, 131.21, 130.07, 128.81, 128.18, 127.80, 125.18, 123.47, 86.50, 52.76; Anal. calcd for $C_{21}H_{15}Cl_2N_3O_2$ (412.27): C, 61.18; H, 3.67; N, 10.19, found C, 61.30; H, 3.51; N, 10.28.

5-(4-Chlorophenyl)-5-hydroxy-3-(4-methoxyphenyl)-4,5-dihydro-1*H*-pyrazol-1-yl (pyridin-3-yl)methanone 6h Colorless solid; yield (2.45 g, 60%); mp 195–197 °C; IR (KBr) $\tilde{\upsilon}$ (cm^{-1}): 3305.13 (OH), 3020.99 (Ar–H), 1703.54 (C=O), 1591.84 (C=N), 1535.58 (C=C); ^{1}H NMR (DMSO-d_6) δ: 8.97 (*s*, 1H, OH; exchangeable with D_2O), 8.77 (*s*, 1H, pyridyl-H-2), 8.17 (*d*, 1H, $J=4$ Hz, pyridyl-H-6), 7.91 (*d*, 1H, $J=8$ Hz, pyridyl-H-5), 7.86 (*d*, 1H, $J=2$ Hz, pyridyl-H-4), 7.73 (*d*, 2H, $J=8$ Hz, Ar–H), 7.58 (*d*, 2H, $J=8$ Hz, Ar–H), 7.40 (*d*, 2H, $J=8$ Hz, Ar–H), 7.33 (*d*, 2H, $J=8$ Hz, Ar–H),3.70 (*d*, 1H, $J=20$ Hz, pyrazoline-CH_2), 3.56 (*d*, 1H, $J=20$ Hz, pyrazoline-CH_2); ^{13}C NMR (DMSO-d_6) δ: 165.80, 156.56, 152.21, 151.87, 145.76, 138.25, 136.50, 134.56, 133.47, 130.07, 129.81, 128.25, 126.50, 125.18, 122.47, 81.47, 52,21, 50.60; Anal. calcd for $C_{22}H_{18}ClN_3O_3$ (407.17): C, 64.79; H, 4.45; N, 10.30, found C, 64.62; H, 4.32; N, 10.19.

Antihyperlipidemic activity

Animals

Forty-two male adult Wistar albino rats weighing 170 ± 10 g have been used. Animals were obtained from the animal house Faculty of Science, Sohag University, Egypt, and fed on the standard diet of commercial rat chow and tap water. Rats were left to acclimatize to the environment for one week prior to inclusion in the experiment. Rats were maintained under standard laboratory conditions at an ambient temperature of 25 ± 2 °C, with 12-h light/12-h dark cycles. Animals were given a free access to food and water up to 24 h prior to their use. This study was approved by the Institutional Animal Care and Use Ethical Committee of Faculty of Medicine, Sohag University.

Experimental protocol

Induction of hyperlipidemia Hyperlipidemia was induced by feeding the rats with high cholesterol diet (HCD) prepared by mixing normal rodent chow with 4% cholesterol and 1% cholic acid (w/w) (Sigma, USA) for 30 successive days [27].

Treatment Rats were randomly divided into seven groups each containing six animals. In group I, normal control was fed a standard diet and orally received 0.5% carboxymethyl cellulose (CMC) as a drug vehicle. The remaining six groups received HCD for 30 days. Group II is hyperlipidemic control and orally received (CMC) 0.5% as a drug vehicle; group III was treated with gemfibrozil orally in a dose of 20 mg/kg per day as a standard hypolipidemic drug [32]. Rats in groups IV, V, VI and VII that received compounds 1, 2, 4 and 5, respectively, in a dose of 20 mg/kg/day orally (1/10 of LD50 dose) were previously determined according to the method of Lorke [28]. The treatment in the last six groups was commenced 15 days after the start of induction of hyperlipidemia and continued for a duration of 15 days [27].

Sample collection and biochemical analysis At the end of the experimental period, rats of all groups were fasted for 16 h and killed by cervical dislocation and blood samples were collected. Serum was separated by centrifugation at 3000 rpm for 10 min at 4 ºC and kept at -20ºC until the time of analysis. Estimation of total cholesterol (TC), triglycerides (TGs), and high-density lipoprotein cholesterol (HDL-C) levels was done by commercially available diagnostic kits (Randox, UK) using Jenway UV–Vis spectrophotometer (Jasco spectrophotometer, USA). The procedure was conducted according to the manufacturer's description, and the concentrations of TC, TGs, and HDL-C were expressed in mg/dl. Serum low-density lipoprotein cholesterol (LDL-C) concentration was determined according to Friedewald's formula [33].

Statistical analysis In the present experimental work, differences between control and treatment groups were analyzed by one way analysis of variance (ANOVA) using "graph Pad Prism version 4.0." All values are given as mean ± standard deviation (SD) of mean. Differences were considered to be significant at $P < 0.05$.

Molecular docking studies Docking of the synthesized compounds was done on the active site of Niemann–Pick C1-Like 1 (NPC1L1) protein (PDB code: 3QNT) using Molecular Orbital Environment software (MOE 2014.0901). Compounds were constructed using the builder interface followed by energy minimization to a

RMSD (root mean square deviations) gradient of 0.01 kcal/mol and RMS (root mean square) distance of 0.1 Å. Forcefield and the partial charges were automatically fixed with MMFF94X (Merck molecular force field 94×). Target protein X-ray crystallographic structure was downloaded from protein data bank (www.rcsb.org). Target structure was prepared by adding hydrogen atoms, automatically correcting atom connection and type. Active site is isolated, and receptor was fixed and docking of the designed compounds is done into the 3D structure of the catalytic site. The obtained poses were studied, and the poses that showed the best ligand–enzyme interactions were selected and stored for energy calculations.

Compliance with ethical standards

Conflict of interest The authors declare that they have no conflict of interest.

References

1. Asija R, Singh C (2016) A comprehensive review on antihyperlipidemic activity of various a comprehensive review on antihyperlipidemic activity of various medicinal plants. Int J Curr Pharm Rev Res 7:407–415
2. Shattat GF (2014) A review article on hyperlipidemia: types, treatments and new drug targets. Biomed Pharmacol J 7:399–409. https://doi.org/10.13005/bpj/504
3. Jain KS, Kathiravan MK, Somani RS, Shishoo CJ (2007) The biology and chemistry of hyperlipidemia. Bioorganic Med Chem 15:4674–4699. https://doi.org/10.1016/j.bmc.2007.04.031
4. Luijten J, van Greevenbroek MMJ, Schaper NC, Meex SJR, van der Steen C, Meijer LJ, de Boer D, de Graaf J, Stehouwer CDA, Brouwers MCGJ (2019) Incidence of cardiovascular disease in familial combined hyperlipidemia: a 15-year follow-up study. Atherosclerosis 280:1–6. https://doi.org/10.1016/j.atherosclerosis.2018.11.013
5. Bodor ET, Offermanns S (2008) Nicotinic acid: an old drug with a promising future. Br J Pharmacol 153:68–75. https://doi.org/10.1038/sj.bjp.0707528
6. Rozman D, Monostory K (2010) Perspectives of the non-statin hypolipidemic agents. Pharmacol Ther 127:19–40. https://doi.org/10.1016/j.pharmthera.2010.03.007
7. Grundy SM, Cleeman JI, Merz CNB, Brewer HB, Clark LT, Hunninghake DB, Pasternak RC, Smith SC (2007) Downloaded from circ.ahajournals.org at BIBLIOTHEQUE CENTRE DE DOC on November 23, 2007, Trial. https://doi.org/10.1161/01.CIR.0000133317.49796.0E
8. Kamanna VS, Kashyap ML (2008) Mechanism of action of niacin. Am J Cardiol 101:20–26. https://doi.org/10.1016/j.amjcard.2008.02.029
9. Chow DC, Tasaki A, Ono J, Shiramizu B, Souza SA (2008) Effect of extended-release niacin on hormone-sensitive lipase and lipoprotein lipase in patients with HIV-associated lipodystrophy syndrome. Biol Targets Ther 2:917–921
10. Ganji SH, Tavintharan S, Zhu D, Xing Y, Kamanna VS, Kashyap ML (2004) Niacin noncompetitively inhibits DGAT2 but not DGAT1 activity in HepG2 cells. J Lipid Res 45:1835–1845. https://doi.org/10.1194/jlr.M300403-JLR200
11. Quackl G, Puglisi L, Schatton W, Schwaier A (1987) Evaluation of hypolipidemic and other useful pharmacological properties of various nicotinic acid derivatives. Drugs Affect Lipid Metab. https://doi.org/10.1017/CBO9781107415324.004
12. Hotz W (1983) Nicotinic acid and its derivatives: a short survey. Adv Lipid Res 20:195–217
13. Goel H, Dunbar RL (2016) Niacin alternatives for dyslipidemia: fool's gold or gold mine? Part II: novel niacin mimetics. Curr Atheroscler Rep 18:1–13. https://doi.org/10.1007/s11883-016-0570-9
14. Bai Z, Zhang J, Zhang Q, Wang Y, Li J, Zhao Q, Wang Z, He D, Zhang J, Liu B (2019) Anti-atherosclerosis effect of H_2S donors based on nicotinic acid and chlorfibrate structures. Bioorganic Med Chem 27:3307–3318. https://doi.org/10.1016/j.bmc.2019.06.012
15. Yu L, Jia L, Betters JL (2011) Niemann-pick C1-like 1 (NPC1L1) protein in intestinal and hepatic cholesterol transport. Annu Rev Physiol 73:239–259. https://doi.org/10.1146/annurev-physiol-012110-142233
16. Davis HR, Altmann SW (2009) Niemann-pick C1 Like 1 (NPC1L1) an intestinal sterol transporter. Biochim Biophys Acta-Mol Cell Biol Lipids 1791:679–683. https://doi.org/10.1016/j.bbalip.2009.01.002
17. Hernandez LMR, de Mejia EG (2017) Bean peptides have higher in silico binding affinities than ezetimibe for the N-terminal domain of cholesterol receptor Niemann-Pick C1 Like-1. Peptides 90:83–89. https://doi.org/10.1016/j.peptides.2017.02.011
18. Sugizaki T, Watanabe M, Horai Y, Kaneko-Iwasaki N, Arita E, Miyazaki T, Morimoto K, Honda A, Irie J, Itoh H (2014) The niemann-pick C1 like 1 (NPC1L1) inhibitor ezetimibe improves metabolic disease via decreased liver X receptor (LXR) activity in liver of obese male mice. Endocrinology 155:2810–2819. https://doi.org/10.1210/en.2013-2143
19. Ge L, Qi W, Wang L, Miao H, Qu Y, Li B, Song B (2011) Flotillins play an essential role in Niemann-Pick C1-like 1-mediated cholesterol uptake. Proc Natl Acad Sci 108:551–556. https://doi.org/10.1073/pnas.1014434108
20. Viegas-Junior Claudio, Barreiro Eliezer J, Fraga Carlos Alberto Manssour, Hybridization Molecular (2007) A useful tool in the design of new drug prototypes. Curr Med Chem 14:1829–1852. https://doi.org/10.2174/092986707781058805
21. Ivasiv V, Albertini C, Goncalves AE, Rossi M, Bolognesi ML (2019) Molecular hybridization as a tool for designing multitarget drug candidates for complex diseases. Curr Top Med Chem 19:1694–1711. https://doi.org/10.2174/1568026619666190619115735
22. Sreedhar NY, Jayapal MR, Sreenivasa Prasad K, Reddy Prasad P (2010) Synthesis and characterization of 4-hydroxy chalcones using PEG-400 as a recyclable solvent. Res J Pharm Biol Chem Sci 1:480–485
23. Ritter M, Martins RM, Rosa SA, Malavolta JL, Lund RG, Flores AFC, Pereira CMP (2015) Green synthesis of chalcones and microbiological evaluation. J Braz Chem Soc 26:1201–1210. https://doi.org/10.5935/0103-5053.20150084
24. Govindaraju M, Mylarappa BN, Ajay Kumar K (2013) Synthesis of novel pyrazole derivatives and their efficacy as antimicrobial agents. Int J Pharm Pharm Sci 5:734–737
25. Kumar A, Jamir L, Sinha UB (2014) Solvent-free dibrominations of alkenes and & #x03B1;,β-unsaturated carbonyl compounds using cetyltrimethyl ammonium tribromide. Chem Sci Trans. https://doi.org/10.7598/cst2014.723
26. Karthikeyan MS, Holla BS, Kumari NS (2007) Synthesis and antimicrobial studies on novel chloro-fluorine containing hydroxy

pyrazolines. Eur J Med Chem 42:30–36. https://doi.org/10.1016/j.ejmech.2006.07.011
27. Sudhahar V, Kumar SA, Sudharsan PT, Varalakshmi P (2007) Protective effect of lupeol and its ester on cardiac abnormalities in experimental hypercholesterolemia. Vascul Pharmacol 46:412–418. https://doi.org/10.1016/j.vph.2006.12.005
28. Lorke D (1983) A new approach to practical testing. Arch Toxicol 54:275–287
29. Minhajuddin M, Beg ZH, Iqbal J (2005) Hypolipidemic and antioxidant properties of tocotrienol rich fraction isolated from rice bran oil in experimentally induced hyperlipidemic rats. Food Chem Toxicol 43:747–753. https://doi.org/10.1016/j.fct.2005.01.015
30. Batra S, Bhaduri AP, Joshi BS, Roy R, Khanna AK, Chander R (2001) Syntheses and biological evaluation of alkanediamines as antioxidant and hypolipidemic agents. Bioorganic Med Chem 9:3093–3099. https://doi.org/10.1016/S0968-0896(01)00185-7
31. Arya N, Dwivedi J, Khedkar VM, Coutinho EC, Jain KS (2013) Design, synthesis and biological evaluation of some 2-azetidinone derivatives as potential antihyperlipidemic agents. Arch Pharm (Weinheim) 346:872–881. https://doi.org/10.1002/ardp.201300262
32. Larsen ML, Illingworth DR, O'Malley JP (1994) Comparative effects of gemfibrozil and clofibrate in type III hyperlipoproteinemia. Atherosclerosis 106:235–240. https://doi.org/10.1016/0021-9150(94)90128-7
33. Friedewald WT, Levy RI, Fredrickson DS (1972) Estimation of the concentration of low-density lipoprotein cholesterol in plasma, without use of the preparative ultracentrifuge. Clin Chem 18:499–502